

Review

Considerations on Possible Directions for a Wide Band Polarimetry X-ray Mission

Paolo Soffitta ^{1,*}, Enrico Costa ^{1,*}, Nicolas De Angelis ¹, Ettore Del Monte ¹, Klaus Desch ²,
Alessandro Di Marco ¹, Giuseppe Di Persio ¹, Sergio Fabiani ¹, Riccardo Ferrazzoli ¹, Markus Gruber ²,
Takahashi Hiromitsu ³, Saba Imtiaz ^{1,4}, Philip Kaaret ⁵, Jochen Kaminski ², Dawoon E. Kim ^{1,6,7},
Fabian Kislat ⁸, Henric Krawczynski ⁹, Fabio La Monaca ^{1,6,7}, Carlo Lefevre ¹, Hemanth Manikantan ¹,
Herman L. Marshall ¹⁰, Romana Mikusincova ¹, Alfredo Morbidini ¹, Fabio Muleri ¹, Stephen L. O'Dell ⁵,
Takashi Okajima ¹¹, Mark Pearce ^{12,13}, Vladislavs Plesanovs ², Brian D. Ramsey ⁵, Ajay Ratheesh ¹,
Alda Rubini ¹, Shraavan Vengalil Menon ⁹ and Martin C. Weisskopf ⁵

- ¹ INAF-Istituto di Astrofisica e Planetologia Spaziali Via Fosso del Cavaliere 100, 00133 Rome, Italy; nicolas.deangelis@inaf.it (N.D.A.); etторе.delmonte@inaf.it (E.D.M.); alessandro.dimarco@inaf.it (A.D.M.); giuseppe.dipersio@inaf.it (G.D.P.); sergio.fabiani@inaf.it (S.F.); riccardo.ferrazzoli@inaf.it (R.F.); saba.imtiaz@inaf.it (S.I.); dawoon.kim@inaf.it (D.E.K.); fabio.lamonaca@inaf.it (F.L.M.); carlo.lefevre@inaf.it (C.L.); hemanth.manikantan@inaf.it (H.M.); romana.mikusincova@inaf.it (R.M.); alfredo.morbidini@inaf.it (A.M.); fabio.muleri@inaf.it (F.M.); ajay.ratheesh@inaf.it (A.R.); alda.rubini@inaf.it (A.R.)
- ² Physikalisches Institut, der Universität Bonn, Nussallee 12, 53115 Bonn, Germany; desch@physik.uni-bonn.de (K.D.); gruber@physik.uni-bonn.de (M.G.); kaminski@physik.uni-bonn.de (J.K.); vladislavs.plesanovs@uni-bonn.de (V.P.)
- ³ Graduate School of Advanced Science and Engineering, Hiroshima University, 1-3-1, Kagamiyama, Higashi-Hiroshima 739-8526, Japan; hrtk@hiroshima-u.ac.jp
- ⁴ Dipartimento di Fisica e Astronomia “Galileo Galilei”, Università degli Studi di Padova, Via VIII febbraio 2, 35122 Padova, Italy
- ⁵ NASA Marshall Space Flight Center, 320 Sparkman Drive, Huntsville, AL 35805, USA; steve.o’dell@nasa.gov (S.L.O.); brian.d.ramsey@nasa.gov (B.D.R.); martin.c.weisskopf@nasa.gov (M.C.W.)
- ⁶ Dipartimento di Fisica, Università degli Studi di Roma “La Sapienza”, Piazzale Aldo Moro 5, 00185 Roma, Italy
- ⁷ Dipartimento di Fisica, Università degli Studi di Roma “Tor Vergata”, Via della Ricerca Scientifica 1, 00133 Roma, Italy
- ⁸ Department of Physics and Astronomy and Space Science Center, University of New Hampshire, Morse Hall, 8 College Rd, Durham, NH 03824, USA; fabian.kislat@unh.edu
- ⁹ Physics Department, Washington University in Saint Louis, 1 Brookings Dr, St. Louis, MO 63130, USA; krawcz@wustl.edu (H.K.); s.vengalilmenon@wustl.edu (S.V.M.)
- ¹⁰ Massachusetts Institute of Technology, 77 Massachusetts Ave, Cambridge, MA 02139, USA; hermanm@mit.edu
- ¹¹ NASA Goddard Space Flight Center, 8800 Greenbelt Rd, Greenbelt, MD 20771, USA; takashi.okajima@nasa.gov
- ¹² KTH Royal Institute of Technology, Department of Physics, 106 91 Stockholm, Sweden; pearce@kth.se
- ¹³ The Oskar Klein Centre for Cosmoparticle Physics, AlbaNova University Centre, 106 91 Stockholm, Sweden
- * Correspondence: paolo.soffitta@inaf.it (P.S.); enrico.costa@inaf.it (E.C.)



Citation: Soffitta, P.; Costa, E.; De Angelis, N.; Del Monte, E.; Desch, K.; Di Marco, A.; Di Persio, G.; Fabiani, S.; Ferrazzoli, R.; Gruber, M.; et al. Considerations on Possible Directions for a Wide Band Polarimetry X-ray Mission. *Galaxies* **2024**, *12*, 47. <https://doi.org/10.3390/galaxies12040047>

Academic Editor: Margo Aller

Received: 30 June 2024

Revised: 28 July 2024

Accepted: 31 July 2024

Published: 8 August 2024



Copyright: © 2024 by the authors. Licensee MDPI, Basel, Switzerland. This article is an open access article distributed under the terms and conditions of the Creative Commons Attribution (CC BY) license (<https://creativecommons.org/licenses/by/4.0/>).

Abstract: The Imaging X-ray Polarimetry Explorer (IXPE) has confirmed that X-ray polarimetry is a valuable tool in astronomy, providing critical insights into the emission processes and the geometry of compact objects. IXPE was designed to be sensitive in the 2–8 keV energy range for three primary reasons: (1) celestial X-ray sources are bright within this range, (2) the optics are effective, and (3) most sources across various classes were expected to exhibit some level of polarization. Indeed, IXPE is a great success, and its discoveries are necessitating the revision of many theoretical models for numerous sources. However, one of IXPE’s main limitations is its relatively narrow energy band, coupled with rapidly declining efficiency. In this paper, we will demonstrate the benefits of devising a mission focused on a broader energy band (0.1–79 keV). This approach leverages current technologies that align well with theoretical expectations and builds on the successes of IXPE.

Keywords: X-rays; astronomy; polarimetry

1. What after IXPE and Why

In the following, we will briefly outline the motivation for a new X-ray polarimetry mission, discussing the strengths and weaknesses of IXPE.

1.1. General Consideration

IXPE [1–3] has opened a new window in astrophysics by providing precise X-ray polarimetry for a diverse sample of celestial sources. Both radio quiet and radio loud AGNs, as well as galactic black hole binaries and neutron stars, have been probed. For the first time, polarization maps in X-rays of pulsar wind nebulae and supernova remnants have been made available. Additionally, faint extended sources, such as molecular clouds and filaments around the Galactic Center and near lobes from microquasars, have been successfully investigated. Although theoretical models were sometimes confirmed, IXPE has reported, for many observations, unexpected results that warrant further and deeper investigation by theorists on one hand and, on the other, a new mission with improved polarimetric capabilities. In this review, we will propose some possible new directions for the second case.

1.2. Strength and Weakness of IXPE and Some Potential Improvement

One of the keys to the success of IXPE is its imaging capabilities, which are invaluable for angularly resolved polarimetry of extended sources but also very effective in keeping background counts at an acceptable level for dim sources. Given the current limitations, it is virtually impossible to use a solid-state detector for photoelectric polarimetry in the near future. The main challenges are the unfavorable small photoelectron track length relative to the available pixel size and the depletion layer. Therefore, gas devices with centimeter-thick absorption/drift regions will still be required. The angular resolution of IXPE, between 25'' and 30'', was only fully utilized for the Crab Pulsar Wind Nebula [4] due to the large statistical requirements for polarimetry and the relatively small effective area of the mirrors. Replicating the exquisite angular resolution of Chandra is a difficult task; however, mirrors with angular resolutions between 5'' and 10'' and effective areas in the range of a few thousand cm² are already becoming accessible. Technological advances include silicon multi-pore optics as well as optics developed using replica techniques.

We have already demonstrated that the half energy width (HEW) of the telescope is primarily determined by the quality of the optics, while the secondary factor is the inclined penetration within the detector's drift length. In fact, with focal lengths in the range of 10–12 m, the degradation due to inclined penetration is modest, and the HEW can be maintained very close to 5''–6'' [5].

The efficiency of an X-ray imaging polarimetry device comes at the expense of the modulation factor because the larger the drift length, the greater the quantum efficiency, but the greater the diffusion as well, which blurs the track and reduces the modulation. However, ASICs of the new generation provide simultaneous information on both energy and arrival time on each pixel. This allows for 3-D imaging of tracks, with an expected increase in the modulation factor. Additionally, new gas-multiplication technologies can improve the energy resolution of gas pixel detectors. A better resolution twice that of IXPE should be feasible. This would benefit the study of supernovae remnants by allowing the resolution of thermal emission lines and excluding them from the analysis, and it would enhance spectro-polarimetric studies of Fe K-alpha lines by resolving lines, the continuum, and the edge.

However, the main limitation of IXPE, which should drive the design of future missions dedicated to polarimetry, is its relatively narrow energy band. This limitation arises from the intrinsic energy-dependent photoelectric cross-section. IXPE's results have demonstrated the advantages of developing a polarimeter with a wider energy band, as will be discussed in the subsequent paragraphs of this review (see also [2,6]). Most of the necessary

technological advancements have already been made or are currently under development, with further progress expected in the near term.

2. Polarimetry below 2 keV

The astrophysics goals for polarimetry below 2 keV are highly compelling, as described below, and they warrant pursuit through a dedicated experiment. In this energy band, the photoelectric effect can be marginally exploited, along with techniques based on Bragg diffraction.

2.1. Scientific Motivation

Some classes of sources are outstanding in the soft range <0.6 keV. E.g., isolated pulsars have a spectrum peaking at 0.1–0.3 keV, where their flux is orders of magnitude larger than in the IXPE range. Among the approximately 1800 rotation-powered pulsars, about 100 are known to emit thermal X-rays with temperatures ranging from 10^5 to 10^6 K, thus peaking at very soft X-ray energies. Non-zero X-ray polarization, expected due to the high magnetic field strengths (see, for example, [7]), can provide insights into geometrical parameters and emission regions. Further, isolated neutron stars, including magnetars, often exhibit thermal emission from their surfaces peaking around or below 1 keV. Notably, about 10 cataloged magnetars are situated at high galactic latitudes. So far, IXPE has observed 4 magnetars with a net observing time in the range of 10^6 s, revealing complex morphology and physical properties of their emission regions from the neutron star surfaces (see, for example, [8]) and magnetosphere. The long-sought QED effect of vacuum birefringence has not yet been unambiguously proven, requiring the detection of significant polarization in their phase-resolved spectra associated with large emitting regions spotted by a very low pulsed fraction emission. Increasing the sample in this energy band would permit better constraints on their complex emission regions, further paving the way to test this elusive QED effect. Among black hole binaries, about a dozen are located at high galactic latitudes. A black hole in a high-soft state emits thermally (peaking in the keV range) from the accretion disk, with possibly extension to the innermost stable circular orbit (ISCO). The low-energy measurements can constrain accretion disk magnetic fields by observing ($E < 1$ keV) the effects of Faraday rotation and depolarization [9]. For some systems, the low-energy polarization will constrain the accretion disk orientation further away from the black hole, and may thus lead to the discovery of warped accretion disks. The most visible blazars are located at high galactic latitudes. High synchrotron peaked blazars (HSP) may have their peak energy in the 0.1 keV to 10 keV range, with very steep power-law indices. IXPE demonstrated that X-ray polarization could be 2–3 times greater at optical, infrared, or mm wavelengths, probing locations with more turbulent magnetic fields (see, for example, [10]). For instance, in the case of Mrk 421, IXPE detected [11] a rapid rotation of the polarization angle in X-rays that was not accompanied by a rotation at longer wavelengths. A measurement in the soft X-ray band would probe whether a smooth transition of these behaviors exists while investigating different magnetic field configurations.

As a matter of fact, while the energy range below 2 keV offers limited sensitivity for all sources located along the galactic plane due to interstellar extinction, it is particularly beneficial, as shown above, for sources located at high galactic latitudes.

2.2. Soft X-ray Gas Photoelectric Imager

Exploiting the photoelectric effect below 2 keV becomes increasingly difficult because the range of the photoelectrons shortens rapidly. The use of a rarefied gas mixture based on, e.g., isobutane, can provide some sensitivity below 1 keV for imaging polarimetry and was studied in the past [12] for potential inclusion in the XEUS-ESA mission (see Figure 1). In fact, the decrease in pressure (P) is accompanied by an increase in diffusion as $\sim \sqrt{d_l/P}$, requiring a short drift length (d_l). Since the range of a photoelectron for sensitive polarimetry must not be much different in each energy band, a possible drawback of this

configuration with a small gas gap (0.5 cm or smaller) could be a larger fraction of events with incomplete charge collection.

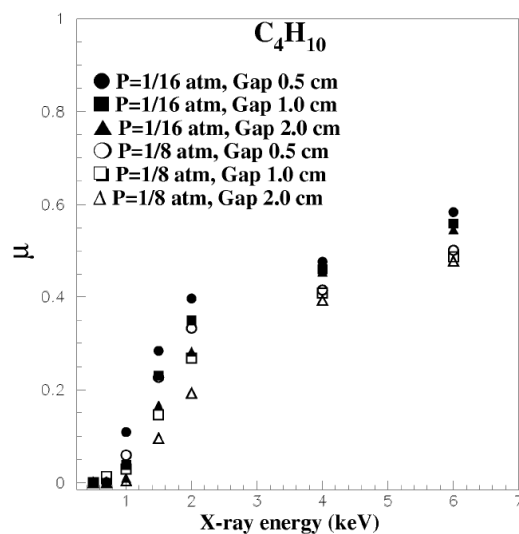


Figure 1. The modulation factor from [12] for some low-pressure gas pixel detectors filled with isobutane as evaluated by Monte Carlo simulation.

Helium is characterized by a large diffusion coefficient and must be used with a gas quencher. Given the K-shell energy of carbon in hydrocarbons, a sensitivity lower limit of about 600 eV must be set, which is due to the presence of polarization-insensitive Auger electrons. With the above constraints, such a device would be virtually transparent above 2 keV. The use of a thin silicon-nitride window will provide better sensitivity compared to polypropylene or polyimide windows, especially at lower energies.

2.3. Graded Multilayer Mirrors

The Bragg technique, despite the large modulation, was heavily limited by the very narrow energy band, which was mitigated by the mosaic technique, and by the limited choice of natural crystals that typically diffract at 45° in the 2–8 keV band. The introduction of artificial organic crystals allowed them to operate in the soft energy range, while the graded thickness increased the bandwidth and hence the efficiency, opening the window of polarimetry for soft X-rays. These materials are also suitable to be used in combination with optics. The most advanced approach was designed [13–16] by using laterally graded artificial multilayer mirrors (LGML) that diffract X-rays dispersed according to their wavelengths by means of a transmission grating. The nearly 45° reflected radiation is detected by a CCD along the grading direction. As a non-dispersive polarimeter, three such devices are necessary to measure the three Stokes parameters I, Q, and U, or one can rotate one device at the expense of sensitivity, especially to variable sources. To achieve the necessary sensitivity, the grating is placed close to an X-ray mirror. The main advantages of such an approach are: (1) a wide soft-energy band anticipated to range from 0.1 to 0.7 keV; (2) a large modulation factor (approaching $\sim 100\%$) across the entire band; (3) very good energy resolution due to the dispersing technique, which may be beneficial in the presence of low-energy lines; (4) a geometric arrangement that allows for designing a stacked instrument (see section Figure 2), with only a small loss of effective mirror area at higher energies; (5) by correlating the signal amplitude with its position on the CCD, the background can be minimized. The proposed instrument relies on laboratory studies of individual components performed at MIT ([17,18]) and simulations of performance ([19]). A rocket demonstrator, REDSoX (Rocket Experiment Demonstrator of a Soft X-ray Polarimeter), has already been funded for flight in a few years, paving the way for an extended version for a dedicated satellite, which is also under study (Globe Observatory Soft X-ray Polarimeter or GoSOX). The estimated

requirement for pointing precision is about 5–7 arcsec [15]. The satellite version requires rotation ($1^\circ/s$) and hosts a single device, whereas the rocket configuration, in principle, does not require rotation if the response to polarized and unpolarized radiation of each of the three devices is sufficiently equalized and well-calibrated.



Figure 2. The REDSoX Rocket Experiment Demonstrator of a Soft X-ray polarimeter. The payload consists of the X-ray optics with Wolter type I mirror shells, 200 nm period critical angle transmission (CAT) gratings mounted on a 2.5 m focal length optical bench. A rocket flight was granted funding to completion. The target for this short flight will be decided with careful evaluation of its real performances.

3. Classical Energy Band 2–10 keV

The classical energy band of X-ray astronomy is benefiting from the results of IXPE and the wealth of theoretical work stemming from its observations. In the following, we will describe how an improved, higher-throughput mission, building upon IXPE's results, will extend polarimetry to a larger number of sources and enhance precision for extended sources.

3.1. Scientific Motivation

For most classes of X-ray emitting sources, IXPE has detected to date polarization from only a handful of bright objects. It observed about a dozen only for bright black-hole and neutron star binary systems. This energy band has the advantage of being much less affected by interstellar absorption. An increase in the mirror's effective area by a factor of approximately 10 would accordingly increase the number of extragalactic sources, especially Seyfert-1 galaxies, where the main primary emission in this energy band is due to Comptonization from the hot corona. This also applies to low synchrotron peaked (LSP) blazars, for which IXPE has detected to date only upper limits, while positive secure multi-wavelength detection can clarify the nature of accelerated particles (leptons or hadrons, [20]). Additionally, HSP blazars can benefit from a larger effective area, which will facilitate studies of polarization variability and its relation to the magnetic field directions within the jet. For these, IXPE has so far only shown the tip of the iceberg [21]. An improvement in angular resolution by a factor of approximately 3–6 will also allow for more detailed exploration of the morphology of pulsar wind nebulae, significantly aiding pulsar polarimetry after IXPE's secure detection in only their brightest phase bins (see, for example, [4]) and only for two of the five observed so far. Considering the dimmest PWN observed by IXPE and the 2010 catalog of Chandra PWN [22], we expect at least an additional 7 PWNs to be within the reach of such an improved mission. Albeit this energy band is non-optimal for studying SNRs, the advantage of a better angular resolution, if accompanied by an increased effective area, would allow to probe turbulence and magnetic field orientation closer to the shock and with higher precision in regions where non-linear diffusive shock acceleration may be at work [23].

3.2. Time Projection Chamber

Following the papers by E. Costa [24] and later by K. Black [25], a significant rejuvenation of X-ray polarimetry in astronomy took place (see Figure 1 in [26]). A few years later, Black [27] devised and built a detector that decoupled the modulation factor from the quantum efficiency, based on the time projection chamber (TPC) approach. The drift

field was perpendicular to the optical axis, and a 1-D readout plane was positioned on a side out of the absorption path. To obtain a 2-D image of the photo-electron track, the timing information from each detected signal is converted into space coordinates using precise knowledge of the drift velocity. The image is good to derive the photoelectron emission angle, but, ignoring the starting time of the drift, the point of interaction cannot be localized. To compensate for the intrinsic systematic effects, the device rotates around the direction of the incoming beam. The main advantage of the TPC is that the drift length and the related diffusion are constant along the depth. A very thick polarimeter with a high detection efficiency is possible. Due to the need to use low-pressure gases the increase in depth with respect to the gas pixel detectors (GPDs) is much larger than what is expected for the increase of efficiency only. The primary drawback of this design is that 1D only imaging does not allow for imaging polarimetry, and the substantial reduction of background amplified by the fact that the blurring due to the absorption of a converging beam on a thick detector is much more substantial than in the GPD. This is not a trivial issue as IXPE showed [28], as (1) the background noise is higher than in an imaging device, and the residual background cannot be subtracted using the same observing time, (2) many celestial objects require imaging for making polarization mapping (supernova remnants [29]), pulsar wind nebulae [30], molecular clouds [31], filaments [32], and lobes of microquasars [33], as shown by IXPE, and (3) the necessity for rotation complicates the study of the polarization pattern from sources showing erratic periodicity, making the use of multiple devices essential.

Although an adequate level of readiness was achieved, constructing a flight device [34] proved more challenging than anticipated. Additionally, the Gravity and Extreme Magnetism SMEX (GEMS) mission [35] was cancelled for programmatic reasons. However, the Time Projection Chamber may be considered for a stacking polarimetric configuration in the future (see Section 5).

3.3. Gas Imager

The gas pixel detector (GPD) [24,36,37], a much-needed but previously lacking tool in this energy range, opened the window of polarimetry in X-ray astronomy. As discussed above, improvements can be envisaged with optics of larger area or better angular resolution, but also with improved detectors by exploiting 3-D track imaging and improving performance in terms of modulation factor and efficiency. Another limitation of the IXPE GPDs was the large dead time (1.1 ms), which is incompatible with the brightest sources and, for sure, with future high-throughput optics. In the Chinese eXTP mission, it will be mitigated by a new XPOL ASIC with a dead time of 0.15 ms [38]. But already with an optics of the order of 1500 cm² (like XMM) and for missions based on new mirror technologies, such as the AXIS mission (4200 cm² on axis [39]), and given the relevance of very bright transient sources, a more substantial improvement is absolutely needed. Another point to address is the intrinsic modulation factor. Optimization over the years, prior to IXPE selection, showed that a 1-cm drift with an 800 mbar dimethyl-ether gas mixture provides the best sensitivity. Although fine-tuning these parameters is based on the energy-dependent mirror effective area and on the source spectrum, no significant change is expected. An improvement in these two areas can come from using the new generation of multipurpose ASICs from the Medipix collaboration, Timepix3 [40] and Timepix4 [41]. They would solve the issue of dead time for any planned high-throughput optics. The Timepix4 could also extend the field of view or preserve the current one, but with a longer focal length. Both record Time-of-Arrival (ToA) and Time-over-Threshold (ToT, proportional to energy) simultaneously in each pixel. ToA information is coded with a nominal resolution of 1.5625 ns (Timepix3) or 195 ps (Timepix4). Timepix3 features 256 × 256 square pixels (55 × 55 μm²) and is virtually dead-time free up to 40 Mhits/cm²/s. The measurement of the ToA for each pixel allows for 3-D track reconstruction, which may lead to a better determination of the photoelectron direction, consequently improving the modulation factor. A possible implementation of such a device as a fine imaging gas detector is GridPix [42,43],

where a metallic mesh onto dielectric pillars 50 μm long provides the multiplication with no additional track diffusion in the transfer gap.

A comparison between the two designs is shown in Table 1. The GPD design shows two major criticalities. One is a rate-dependent decrement of the gain due to the attachment of charges produced in the avalanche onto the gas electron multiplier (GEM). This varies pixel by pixel and is difficult to model or calibrate during flight. The second issue is the absorption (or adsorption) of the gas (dimethyl-ether) by the elements of the GPD body (most probably by the glue). The use of a mesh solves the first issue, but it requires a thin coating of Si_3N_4 onto the ASIC top layer for safety in case of sparking, the effect of which on charging needs still to be evaluated. Other approaches may use a partially conductive, two-sided, metallic, micro-porous lead-glass device in place of the GEM [44].

Table 1. Table of comparison of performances between IXPE GPD and GridPix (with Timepix3 ASIC [40]). In parentheses are the expected performances of XPOL III [38], a new version of the ASIC on-board IXPE.

	GPD	GridPix
Pattern	Hex 50 μm pitch	55 \times 55 μm^2 pitch
Amplitude Signals Output	Analog	Digital (ToT)
Size	1.5 \times 1.5 cm^2	1.4 \times 1.4 cm^2
Track imaging	2-D	3-D
Maximum rate for 10 % dead-time fraction	100 (700)	10^6 (100 pixels track)
Diffusion in Transfer gap (DME, μm_{rms})	55	8
Noise per pixel (e_{rms})	50 (30)	60
Threshold dispersion (e_{rms})	Non equaliz.	35 (equaliz.)
Minimum Threshold (e^-)	2300 (150)	500 (ToT/ToA)

The issue of absorption/adsorption (producing a loss of efficiency of $\sim 20\%$) may be solved with a careful choice of the constructive elements of the detector and, possibly, by replacing DME with another low-diffusion low atomic number gas mixture (isobutane, CO_2). These gas mixtures have similar transverse diffusion with DME, while CO_2 may require a larger electric field for comparable multiplication. Also, it has a larger energy threshold for polarimetry due to the larger amount of oxygen.

Finally, we note that the spurious modulation (the residual modulation from an unpolarized source) was reduced by a readout optimization and eventually corrected with a huge calibration campaign. For GridPix, it is also needed to show that the square geometry and the slightly larger pixel size do not introduce additional spurious modulation or, if this is the case, that it can be modeled and efficiently subtracted.

4. Hard X-ray Band (10–80 keV)

In the following, we will explain how integrating imaging photoelectric X-ray polarimetry with Compton polarimetry, by leveraging the capabilities of multilayer X-ray mirrors, can uncover entirely new phenomena and enable measurements that are challenging to perform in the classical energy band.

4.1. Scientific Motivation

The energy band of IXPE just borders some of the main scientific objectives for polarimetry. We reviewed the most important ones (see also [45]) (1) Reflections in AGNs: above 6 keV, the spectrum of Seyfert-1 galaxies is dominated by reflection (scattering) of primary radiation from the disk, or in Seyfert-2 galaxies, from the scattering from the

ionization cones (warm-reflector) or from the surrounding molecular torus (cold-reflector). IXPE showed that the primary radiation of Seyfert-1 galaxies comes from a corona (slab or wedge-shaped) orthogonal to the disk's normal axis [46]. In the IXPE energy band, the reflection fraction of NGC 4151 is only 8%, doubling in the upper energy band. The polarization of the reflected component (which may provide the geometry of the disk and possibly the black hole's spin) from the disk was not firmly measured. In the reflection-dominated Compton-thick Circinus galaxy, the reflection from the torus was measured [47], albeit the polarization from the ionization cone was largely unconstrained. The same goes for NGC 1068, the archetypal Seyfert-2 galaxy [48]. The possible misalignment between these two structures could be measured ([49]) by efficient X-ray spectro-polarimetry in a wide energy band with deep consequences in the AGN formation and feedback mechanism. IXPE also showed how difficult the 2–8 keV polarimetry of supernova remnants (see, for example, [29]) is due to the presence of lines and large thermal emissions. Imaging polarimetry above iron lines will facilitate the study of synchrotron non-thermal emission and may explain the new features detected in Cas A SNR by NuSTAR [50]. As already mentioned above, IXPE showed a complex pattern for the emission regions from magnetars. Further, INTEGRAL and NuSTAR detected a hard energy tail extending at least up to 100 keV, which does not always appear to be the continuation of the lower energy power law for all the sources [51,52]. Polarimetry in the 6–30 keV energy band will help shed light on their origin by exploring the transition between these two components. Given the faintness of this source imaging, polarimetry is required to reduce the impact of the background. IXPE surprises also come from binary pulsars and their lower-than-expected polarization (see, for example, [53]). While an intense modeling effort is needed, the measurement of polarization at the cyclotron line (fundamental and higher harmonics) is still lacking because almost all the neutron-star binaries are characterized by cyclotron line fundamentals at energies above 10 keV. It is still not clear whether the linear polarization at the energy close to the cyclotron line is large ($\sim 80\%$ [54]) or zero [55,56]. Such measurements would be definitively crucial to characterizing the transport of photons through a magnetized plasma at resonance energy. Finally, IXPE paved the way for making tomography of the galactic center by means of polarimetry of X-rays shining from cold molecular clouds in the galactic center region [31]. However, this is still a low-significance result due to the presence of relatively warm and bright plasma emitting in the few keV energy band. A hard X-ray imaging device ($10''$ – $20''$ HEW) can enable cleaner and more sensitive measurements, expanding the range of molecular clouds for which such measurements are feasible. Consequently, this could help determine the time evolution of the flare.

4.2. Photoelectron Gas Charge Imager (6–35 keV)

A gas photoelectron charge imager sensitive to polarization above 6 keV up to approximately 30 keV requires the use of pressurized Argon as the principal gas [57] with a thick gas cell. A GPD filled with a 2-bar, 2-cm Ar-DME gas mixture has already been built and tested [58], and an implementation (3 cm, 3 bar) for an ESA mission was already proposed [59] with comparable sensitivity to a GPD in the 2–8 keV energy band (see Figure 3). A TPC 7.8 cm thick, was also more recently tested with a 1-bar 60–40 Ar-DME mixture up to 16 keV [60]. In the hard X-ray and soft gamma-ray energy bands, the residual (instrumental) background, mainly due to Earth's albedo, decays with energy with a law less steep than celestial sources, so that the need for good discrimination increases with the energy. A sensitive experiment using a photoelectron gas charge imager necessitates a careful background rejection, through topological analysis of the detected tracks [28] by applying the techniques traditionally applied with proportional counters and not excluding an active anti-coincidence system to reject the minimum ionizing particles (MIPs). All these are viable with GridPix. Last but not least, the imaging capabilities of the GPD and GridPix devices additionally allow for background subtraction simultaneously to the observation by using the same sky image. The background in the focus of an imaging device is the one within the point spread function, orders of magnitude smaller than that of a non-imaging

device. And, most of all, many important scientific cases (a few mentioned above) deserve imaging polarimetry: this is the legacy of IXPE.

The sensitivity of such a broad-band mission can only be accurately determined through a detailed design. However, a rough order of magnitude estimation can provide confidence that such a mission will remain competitive. For the high-energy part, we can reference computations performed nearly 10 years ago when a new hard X-ray mission (NHXM) was proposed to ESA in response to the M3 call [61]. This mission was based on four multilayer telescopes with a focal length of 10 m. Although it was only a design, comparisons of effective areas at different hard X-ray energies show them to be comparable to NuSTAR and XL-Calibur, two existing missions. The sensitivity for the low energy polarimeter (LEP, 2–10 keV) and the medium energy polarimeter (MEP, 5–35 keV) was computed based on simulations and laboratory data [59,61]. The LEP detector is quite similar to IXPE, and the optics effective area is comparable ($\sim 500 \text{ cm}^2$ for NHXM vs. $\sim 600 \text{ cm}^2$ for IXPE). The computed minimum detectable polarization (MDP) for a 0.5 mCrab source in 10 days was 5.1% compared to IXPE's 5.5%. The MDP for the MEP was approximately 34% worse in terms of mCrabs, as shown in Figure 3. A combination of one LEP and two MEPs would be very balanced. We can assume that new ideas for gas detectors, such as 3-D reconstruction, will improve both stages. Therefore, it is reasonable to assume that a combination of LEP and MEP can be well-matched in terms of science and practical for future implementation.

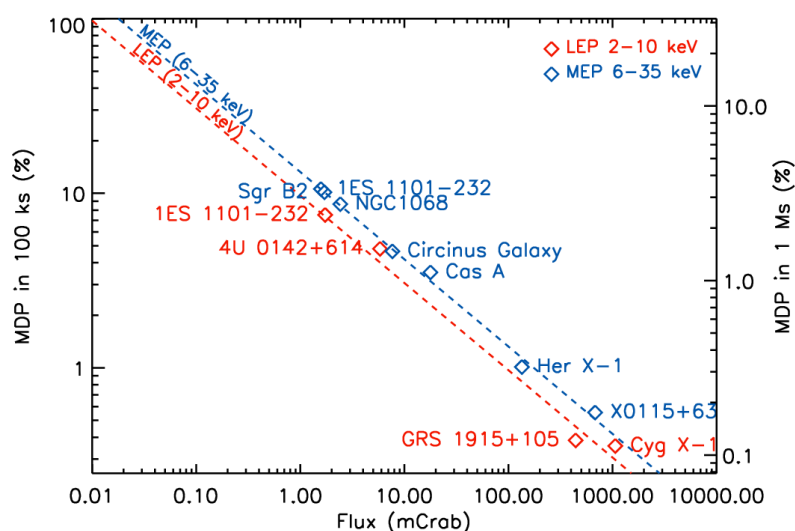


Figure 3. The sensitivity of the LEP (2–10 keV) and MEP (5–35 keV) foreseen for the new hard X-ray mission [61].

4.3. Compton Polarimeter (up to 79 keV)

Above 20 keV, photoelectric polarimetry with Ar-based mixtures starts to compete with Compton polarimetry, with a possible overlap between 20 and 30 keV. The use of mixtures based on krypton still needs to be studied, but could be discouraged by the large fluorescence yield and the large scattering/stopping ratio. Compton polarimeters at the focus of X-ray optics have, until now, only been used in balloon-borne experiments [62,63] and were proposed in the past for both PolariS, a Japanese experiment by JAXA [64] and PolSTAR, a NASA SMEX mission [65]. A focal plane Compton polarimeter requires the use of two phases [66,67]: a scattering phase with a low atomic number scintillator (lithium, beryllium, or plastic [68], organic crystals like p-Terphenyl were found [69] less effective than expected) and an absorber phase. The choice of the scatterer depends on the energy threshold and, consequently, on the active or passive configuration. A passive configuration may have a low energy threshold of 5–6 keV [70] for a satellite or 15–20 keV for a balloon-borne experiment but the background is high, so an efficient active inorganic

anti-coincidence shield is necessary (as for example in XL-Calibur [71] where the focal plane Compton polarimeter is shown in Figure 4).

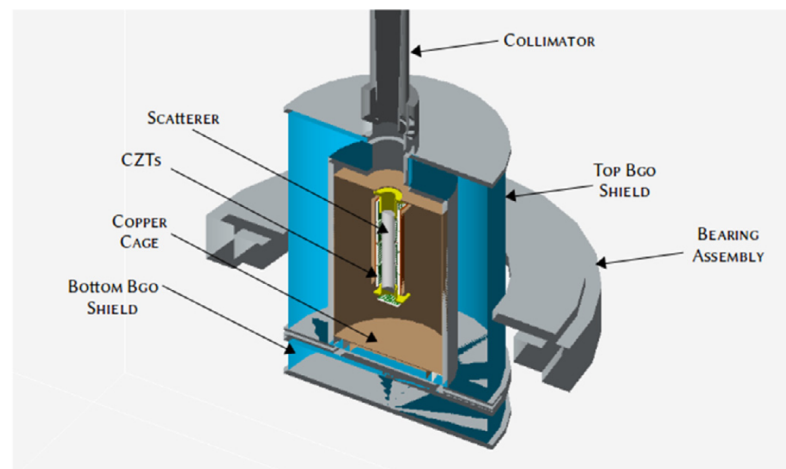


Figure 4. The configuration of the XL-Calibur focal plane instrument. One Beryllium scatterer is surrounded by four planes of CZT detectors, surrounded by a thick BGO shield to reduce the background [72].

In fact, imaging is not possible, nor is it possible to cover a large area for a collimated experiment. An active Compton polarimeter may have a much smaller background just by using the coincidence technique alone. However, the energy threshold for active use is higher (~ 20 keV) even for a satellite focal plane experiment [69,73]. With segmented scatterers with a $\sim 4\text{--}9$ mm² area in an array of 16–36 elements at the focus of ~ 10 m focal plane multilayer optics, coarse imaging of ~ 1 arcmin is possible. Segmentation reduces the impact of off-axis pointing (for passive elements, such impact is explored and mitigated as in [74,75]). This is the configuration proposed for PolariS. For such a configuration, the threshold may be higher due to the aspect ratio of the single plastic scintillator, although sensitivity, even at 20 keV, has been demonstrated [64]. An improved design may take advantage of reading out the signal from both sides of the scatterer and the absorber using two thinned SDDs, two thinned SiPMs, or silicon drift detectors [76]. If proved effective enough, this configuration facilitates the construction of a possible 3-D Compton polarimeter with improved performance in terms of low background, high modulation factor, and sensitivity. A Compton polarimeter allows for extending the band up to the maximum energy permitted by the use of a multilayer mirror. Imaging would also allow mapping of magnetic fields in the Crab PWN and in SNRs up to these energies. Predicting the sensitivity of such an instrument is challenging due to the many variables that need confirmation. In a follow-up to the new hard X-ray mission proposal, the team [59] evaluated the performance of a scattering polarimeter with an active plastic scintillator scatterer and a cylindrical absorber, based on certain assumptions about triggering efficiency and zero background. These factors require validation through simulations, testing, and analysis of XL-Calibur data. However, the computations suggest that reasonable performance could be achieved in this band, with an MDP of 6% for a 1.8 mCrab source. Even though actual trade-offs might worsen this number, we are close to achieving the goal of broad-band polarimetry.

5. A Possible Stacked Configuration

A future sensitive X-ray polarimetry mission should explore the energy band in the 0.1–80 keV range, as previously discussed. Such a mission can be designed either in a multi-instrument configuration with multiple optics optimized for specific energy bands or with a single telescope with a platform to change the instrument at the focal point. The first configuration optimizes the design of the telescope (mirror and detector system) for a

given energy band, while the second minimizes the number of mirrors but is less efficient in covering the whole energy band and does not allow for simultaneous observation across the entire band.

Given the availability of multilayer, high-throughput, fine HEW mirrors, a stacking configuration may optimize available resources to provide sufficient mirror area by replicating the mirror-detector system. A possible stacking configuration has already been proposed [77,78]. It is natural to design a binary-detector system comprising a TPC on top, filled with a DME mixture sensitive on a 2–15 keV range or an Ar-DME mixture to be sensitive to 10–30 keV, coupled, through a thin window (Be) to a scattering polarimeter underneath to extend the band up to 80 keV. This is because, as mentioned, the sensitive plane is parallel to the photon beam.

Unfortunately, the lack of imaging compromises a significant subset of the potential science goals mentioned above. An imaging system with a sensitive plane perpendicular to the photon beam is essential, provided the detector is thin enough to minimize radiation absorption by passive materials, ensuring maximum detection by the active systems. This substrate includes the ASIC chip and the underlying board (and, in the case of GPD, the Kyocera package). For Timepix3, the wafer, initially 800 μm thick, can be thinned down to 180 μm without any loss in performance (Bergmann, B. Czech Technical University in Prague, private communication), resulting in a transparency of 85% at 20 keV. With a thin board or a hole beneath the ASIC and the potential use of a beryllium window, if necessary, a stacked imaging system becomes feasible. The gas stage should be positioned on the focal plane, while the scattering stage can tolerate some defocusing, especially considering the small convergence of hard X-ray optics. An even more ambitious solution could involve three stacked detectors: a front TPC (Time Projection Chamber) tuned to lower energies (1–6 keV), a GridPix for the medium range (6–30 keV), and a scattering stage for higher energies (30–80 keV). These detectors, mounted on a single telescope, could provide the polarimetry capability for a multi-mirror mission in X-ray astronomy.

6. Conclusions

In this review, we demonstrate the advantages of designing an X-ray polarimetry mission that spans the 0.1 keV to 79 keV range. The IXPE mission explored the 2–8 keV energy band, uncovering new opportunities beyond the boundaries of this classical energy band. Current single mirror designs within this range already allow for a threefold increase in sensitivity and a three- to sixfold improvement in angular resolution. At higher energies, focal plane polarimetry has been implemented only through Compton scattering in balloon-borne experiments such as X-Calibur and XL-Calibur, which offer limited sensitivity. However, a satellite mission that effectively combines the imaging photoelectric effect and focal plane Compton scattering will significantly enhance sensitivity, enabling the detection of previously unseen phenomena in the hard X-ray energy band.

Funding: The adaptation of GridPIX detector for X-ray polarimetry is partially supported by the Italian Ministry of Education, University and Research through the project PRIN: Progetti di Ricerca di Rilevante Interesse Nazionale “HypeX: High Yield Polarimetry Experiment in X-rays” (Prot. 2020MZ884C). XL-Calibur is funded in Sweden by Rymdstyrelsen (2022-00178) and Vetenskapsrådet (2021-05128).

Acknowledgments: The Imaging X-ray Polarimetry Explorer (IXPE) is a joint US and Italian mission. The US contribution is supported by the National Aeronautics and Space Administration (NASA) and led and managed by its Marshall Space Flight Center (MSFC), with industry partner Ball Aerospace (contract NNM15AA18C). The Italian contribution is supported by the Italian Space Agency (Agenzia Spaziale Italiana, ASI) through contract ASI-OHBI-2022-13-I.0, agreements ASI-INAF-2022-19-HH.0 and ASI-INFN-2017.13-H0, and its Space Science Data Center (SSDC) with agreements ASI-INAF-2022-14-HH.0 and ASI-INFN 2021-43-HH.0, and by the Istituto Nazionale di Astrofisica (INAF) and the Istituto Nazionale di Fisica Nucleare (INFN) in Italy. This research used data products provided by the IXPE Team (MSFC, SSDC, INAF, and INFN) and distributed with additional software tools by the High-Energy Astrophysics Science Archive Research Center (HEASARC), at NASA Goddard Space

Flight Center (GSFC). PS acknowledges Ministry of Foreign Affairs and International Cooperation (MAECI) contribution 2023-2025 Grant “RES-PUBLICA Research Endeavour for Science Polarimetry with the University of Bonn in Liason with INAF for Cosmic Applications”.

Conflicts of Interest: The authors declare no conflicts of interest.

References

- Weisskopf, M.C.; Soffitta, P.; Baldini, L.; Ramsey, B.D.; O’Dell, S.L.; Romani, R.W.; Matt, G.; Deinger, W.D.; Baumgartner, W.H.; Bellazzini, R.; et al. The Imaging X-ray Polarimetry Explorer (IXPE): Pre-Launch. *J. Astron. Telesc. Instrum. Syst.* **2022**, *8*, 026002. [[CrossRef](#)]
- Soffitta, P.; Baldini, L.; Bellazzini, R.; Costa, E.; Latronico, L.; Muleri, F.; Del Monte, E.; Fabiani, S.; Minuti, M.; Pinchera, M.; et al. The Instrument of the Imaging X-ray Polarimetry Explorer. *Astron. J.* **2021**, *162*, 208. [[CrossRef](#)]
- Baldini, L.; Barbanera, M.; Bellazzini, R.; Bonino, R.; Borotto, F.; Brez, A.; Caporale, C.; Cardelli, C.; Castellano, S.; Ceccanti, M.; et al. Design, construction, and test of the Gas Pixel Detectors for the IXPE mission. *Astropart. Phys.* **2021**, *133*, 102628. [[CrossRef](#)]
- Bucciantini, N.; Ferrazzoli, R.; Bachetti, M.; Rankin, J.; Di Lalla, N.; Sgrò, C.; Omodei, N.; Kitaguchi, T.; Mizuno, T.; Gunji, S.; et al. Simultaneous space and phase resolved X-ray polarimetry of the Crab pulsar and nebula. *Nat. Astron.* **2023**, *7*, 602–610. [[CrossRef](#)]
- Fabiani, S.; Lazzarotto, F.; Bellazzini, R.; Brez, A.; Costa, E.; di Cosimo, S.; Muleri, F.; Rubini, A.; Soffitta, P.; Spandre, G. The Study of PWNe with a photoelectric polarimeter. In Proceedings of the Polarimetry Days in Rome: Crab Status, Theory and Prospects, Rome, Italy, 16–17 October 2008; p. 27. [[CrossRef](#)]
- Krawczynski, H.; Matt, G.; Ingram, A.R.; Taverna, R.; Turolla, R.; Kislat, F.; Teddy Cheung, C.C.; Bykov, A.; Sinha, K.; Zhang, H.; et al. Astro2020 Science White Paper: Using X-ray Polarimetry to Probe the Physics of Black Holes and Neutron Stars. *arXiv* **2019**, arXiv:1904.09313. [[CrossRef](#)]
- Pavlov, G.G.; Zavlin, V.E. Polarization of Thermal X-rays from Isolated Neutron Stars. *Astrophys. J.* **2000**, *529*, 1011–1018. [[CrossRef](#)]
- Taverna, R.; Turolla, R.; Muleri, F.; Heyl, J.; Zane, S.; Baldini, L.; González-Caniulef, D.; Bachetti, M.; Rankin, J.; Caiazzo, I.; et al. Polarized X-rays from a magnetar. *Science* **2022**, *378*, 646–650. [[CrossRef](#)]
- Davis, S.W.; Blaes, O.M.; Hirose, S.; Krolik, J.H. The Effects of Magnetic Fields and Inhomogeneities on Accretion Disk Spectra and Polarization. *Astrophys. J.* **2009**, *703*, 569–584. [[CrossRef](#)]
- Liodakis, I.; Marscher, A.P.; Agudo, I.; Berdyugin, A.V.; Bernardos, M.I.; Bonnoli, G.; Borman, G.A.; Casadio, C.; Casanova, V.; Cavazzuti, E.; et al. Polarized blazar X-rays imply particle acceleration in shocks. *Nature* **2022**, *611*, 677–681. [[CrossRef](#)]
- Di Gesu, L.; Donnarumma, I.; Tavecchio, F.; Agudo, I.; Barnounin, T.; Cibrario, N.; Di Lalla, N.; Di Marco, A.; Escudero, J.; Errando, M.; et al. The X-ray Polarization View of Mrk 421 in an Average Flux State as Observed by the Imaging X-ray Polarimetry Explorer. *Astrophys. J. Lett.* **2022**, *938*, L7. [[CrossRef](#)]
- Pacciani, L.; Costa, E.; Di Persio, G.; Feroci, M.; Soffitta, P.; Baldini, L.; Bellazzini, R.; Brez, A.; Lumb, N.; Spandre, G. Sensitivity of a photoelectric X-ray polarimeter for astronomy: The impact of the gas mixture and pressure. In *Polarimetry in Astronomy, Proceedings of the Astronomical Telescopes and Instrumentation, Waikoloa, HI, USA, 22–28 August 2002*; SPIE: Bellingham, WA, USA, 2003; Volume 4843, p. 394.
- Marshall, H.L.; Schulz, N.S.; Trowbridge Heine, S.N.; Heilmann, R.K.; Günther, H.M.; Egan, M.; Hellickson, T.; Schattenburg, M.; Chakrabarty, D.; Windt, D.L.; et al. The rocket experiment demonstration of a soft X-ray polarimeter (REDSOX Polarimeter). In *Proceedings of the Society of Photo-Optical Instrumentation Engineers (SPIE) Conference Series*; Siegmund, O.H., Ed.; SPIE: Bellingham, WA, USA, 2017; Volume 10397, p. 103970K. [[CrossRef](#)]
- Marshall, H.L.; Günther, H.M.; Heilmann, R.K.; Schulz, N.S.; Egan, M.; Hellickson, T.; Heine, S.N.T.; Windt, D.L.; Gullikson, E.M.; Ramsey, B.; et al. Design of a broadband soft X-ray polarimeter. *J. Astron. Telesc. Instrum. Syst.* **2018**, *4*, 011005. [[CrossRef](#)]
- Marshall, H.L. Analysis of Polarimetry Data with Angular Uncertainties. *Astron. J.* **2021**, *162*, 134. [[CrossRef](#)]
- Marshall, H.L.; Heine, S.; Garner, A.; Masterson, R.; Günther, M.M.; Heilmann, R.; Bongiorno, S.; Gullikson, E.; The Rocket Experiment Demonstration of a Soft X-ray Polarimeter (REDSOX). In Proceedings of the Multifrequency Behaviour of High Energy Cosmic Sources XIV, Palermo, Italy, 12–17 June 2023; Volume 76. Available online: <https://ui.adsabs.harvard.edu/abs/2024mbhe.confE..76M> (accessed on 30 July 2024).
- Garner, A.; Marshall, H.L.; Trowbridge Heine, S.N.; Heilmann, R.K.; Song, J.; Schulz, N.S.; LaMarr, B.J.; Egan, M. Component testing for X-ray spectroscopy and polarimetry. In *Proceedings of the UV, X-ray, and Gamma-Ray Space Instrumentation for Astronomy XXI*; Society of Photo-Optical Instrumentation Engineers (SPIE) Conference Series; Siegmund, O.H., Ed.; SPIE: Bellingham, WA, USA, 2019; Volume 11118, p. 1111811. [[CrossRef](#)]
- Garner, A.; Marshall, H.L.; Trowbridge Heine, S.N.; Heilmann, R.K.; Song, J.; Schulz, N.S.; LaMarr, B.J.; Egan, M. CAT grating alignment and testing for soft X-ray polarimetry. In *Proceedings of the Space Telescopes and Instrumentation 2020: Ultraviolet to Gamma Ray*; Society of Photo-Optical Instrumentation Engineers (SPIE) Conference Series; den Herder, J.W.A., Nikzad, S., Nakazawa, K., Eds.; SPIE: Bellingham, WA, USA, 2020; Volume 11444, p. 114445Z. [[CrossRef](#)]
- Günther, H.M.; Egan, M.; Heilmann, R.K.; Heine, S.N.T.; Hellickson, T.; Frost, J.; Marshall, H.L.; Schulz, N.S.; Theriault-Shay, A. REDSOX: Monte-Carlo ray-tracing for a soft X-ray spectroscopy polarimeter. In *Proceedings of the Society of Photo-Optical*

- Instrumentation Engineers (SPIE) Conference Series*; O'Dell, S.L., Pareschi, G., Eds.; SPIE: Bellingham, WA, USA, 2017; Volume 10399, p. 1039917. [[CrossRef](#)]
20. Zhang, H.; Böttcher, M. X-ray and Gamma-Ray Polarization in Leptonic and Hadronic Jet Models of Blazars. *Astrophys. J.* **2013**, *774*, 18. [[CrossRef](#)]
 21. Kim, D.E.; Di Gesu, L.; Liodakis, I.; Marscher, A.P.; Jorstad, S.G.; Middei, R.; Marshall, H.L.; Pacciani, L.; Agudo, I.; Tavecchio, F.; et al. Magnetic field properties inside the jet of Mrk 421. Multiwavelength polarimetry, including the Imaging X-ray Polarimetry Explorer. *Astron. Astrophys.* **2024**, *681*, A12. [[CrossRef](#)]
 22. Kargaltsev, O.; Pavlov, G.G. Pulsar-wind nebulae in X-rays and TeV γ -rays. In Proceedings of the X-ray Astron. 2009 Present Status Multi-Wavel. Approach Future Perspect, Bologna, Italy, 7–11 September 2009; Volume 1248, pp. 25–28. [[CrossRef](#)]
 23. Bykov, A.M.; Ellison, D.C.; Osipov, S.M.; Pavlov, G.G.; Uvarov, Y.A. X-ray Stripes in Tycho's Supernova Remnant: Synchrotron Footprints of a Nonlinear Cosmic-ray-driven Instability. *Astrophys. J. Lett.* **2011**, *735*, L40. [[CrossRef](#)]
 24. Costa, E.; Soffitta, P.; Bellazzini, R.; Brez, A.; Lumb, N.; Spandre, G. An efficient photoelectric X-ray polarimeter for the study of black holes and neutron stars. *Nature* **2001**, *411*, 662. [[CrossRef](#)]
 25. Black, J.K.; Deines-Jones, P.; Ready, S.; Street, R.E. X-ray polarimetry with an active-matrix pixelproportional counter. *Nucl. Instrum. Methods Phys. Res. A* **2003**, *513*, 639–643. [[CrossRef](#)]
 26. Marin, F. The Growth of Interest in Astronomical X-ray Polarimetry. *Galaxies* **2018**, *6*, 38. [[CrossRef](#)]
 27. Black, J.K.; Baker, R.G.; Deines-Jones, P.; Hill, J.E.; Jahoda, K. X-ray polarimetry with a micropattern TPC. *Nucl. Instrum. Methods Phys. Res. A* **2007**, *581*, 755–760. [[CrossRef](#)]
 28. Di Marco, A.; Soffitta, P.; Costa, E.; Ferrazzoli, R.; La Monaca, F.; Rankin, J.; Ratheesh, A.; Xie, F.; Baldini, L.; Del Monte, E.; et al. Handling the Background in IXPE Polarimetric Data. *Astron. J.* **2023**, *165*, 143. [[CrossRef](#)]
 29. Vink, J.; Prokhorov, D.; Ferrazzoli, R.; Slane, P.; Zhou, P.; Asakura, K.; Baldini, L.; Bucciantini, N.; Costa, E.; Di Marco, A.; et al. X-ray Polarization Detection of Cassiopeia A with IXPE. *Astrophys. J.* **2022**, *938*, 40. [[CrossRef](#)]
 30. Xie, F.; Di Marco, A.; La Monaca, F.; Liu, K.; Muleri, F.; Bucciantini, N.; Romani, R.W.; Costa, E.; Rankin, J.; Soffitta, P.; et al. Vela pulsar wind nebula X-rays are polarized to near the synchrotron limit. *Nature* **2022**, *612*, 658–660. [[CrossRef](#)] [[PubMed](#)]
 31. Marin, F.; Churazov, E.; Khabibullin, I.; Ferrazzoli, R.; Di Gesu, L.; Barnouin, T.; Di Marco, A.; Middei, R.; Vikhlinin, A.; Costa, E.; et al. X-ray polarization evidence for a 200-year-old flare of Sgr A*. *Nature* **2023**, *619*, 41–45. [[CrossRef](#)] [[PubMed](#)]
 32. Churazov, E.; Khabibullin, I.; Barnouin, T.; Bucciantini, N.; Costa, E.; Di Gesu, L.; Di Marco, A.; Ferrazzoli, R.; Forman, W.; Kaaret, P.; et al. Pulsar-wind-nebula-powered Galactic center X-ray filament G0.13-0.11. Proof of the synchrotron nature by IXPE. *Astron. Astrophys.* **2024**, *686*, A14. [[CrossRef](#)]
 33. Kaaret, P.; Ferrazzoli, R.; Silvestri, S.; Negro, M.; Manfreda, A.; Wu, K.; Costa, E.; Soffitta, P.; Safi-Harb, S.; Poutanen, J.; et al. X-ray Polarization of the Eastern Lobe of SS 433. *Astrophys. J. Lett.* **2024**, *961*, L12. [[CrossRef](#)]
 34. Hill, J.E.; Baker, R.G.; Black, J.K.; Browne, M.J.; Baumgartner, W.H.; Caldwell, E.M.; Cantwell, J.D.; Davies, A.; Desai, A.B.; Dickens, P.L.; et al. The design and qualification of the GEMS X-ray polarimeters. In *Proceedings of the Society of Photo-Optical Instrumentation Engineers (SPIE) Conference Series*; SPIE: Bellingham, WA, USA, 2012; Volume 8443. [[CrossRef](#)]
 35. Swank, J.; Kallman, T.; Jahoda, K.; Black, K.; Deines-Jones, P.; Kaaret, P. Gravity and Extreme Magnetism SMEX (GEMS). In *X-ray Polarimetry: A New Window in Astrophysics by Ronaldo Bellazzini, Enrico Costa, Giorgio Matt and Gianpiero Tagliaferri*; Bellazzini, R., Costa, E., Matt, G., Tagliaferri, G., Eds.; Cambridge University Press: Cambridge, UK, 2010; p. 251, ISBN 9780521191845.
 36. Bellazzini, R.; Spandre, G.; Minuti, M.; Baldini, L.; Brez, A.; Cavalca, F.; Latronico, L.; Omodei, N.; Massai, M.M.; Sgro', C.; et al. Direct reading of charge multipliers with a self-triggering CMOS analog chip with 105 k pixels at 50 μm pitch. *Nucl. Instrum. Methods Phys. Res. A* **2006**, *566*, 552. [[CrossRef](#)]
 37. Bellazzini, R.; Spandre, G.; Minuti, M.; Baldini, L.; Brez, A.; Latronico, L.; Omodei, N.; Razzano, M.; Massai, M.M.; Pesce-Rollins, M.; et al. A sealed Gas Pixel Detector for X-ray astronomy. *Nucl. Instrum. Methods Phys. Res. A* **2007**, *579*, 853. [[CrossRef](#)]
 38. Minuti, M.; Baldini, L.; Bellazzini, R.; Brez, A.; Ceccanti, M.; Krummenacher, F.; Latronico, L.; Lucchesi, L.; Manfreda, A.; Orsini, L.; et al. XPOL-III: A new-generation VLSI CMOS ASIC for high-throughput X-ray polarimetry. *Nucl. Instrum. Methods Phys. Res. A* **2023**, *1046*, 167674. [[CrossRef](#)]
 39. Reynolds, C.S.; Kara, E.A.; Mushotzky, R.F.; Ptak, A.; Koss, M.J.; Williams, B.J.; Allen, S.W.; Bauer, F.E.; Bautz, M.; Bogadhee, A.; et al. Overview of the advanced X-ray imaging satellite (AXIS). In *Proceedings of the UV, X-ray, and Gamma-Ray Space Instrumentation for Astronomy XXIII*; Society of Photo-Optical Instrumentation Engineers (SPIE) Conference Series; Siegmund, O.H., Hoadley, K., Eds.; SPIE: Bellingham, WA, USA, 2023; Volume 12678, p. 126781E. [[CrossRef](#)]
 40. Poikela, T.; Plosila, J.; Westerlund, T.; Campbell, M.; De Gaspari, M.; Llopart, X.; Gromov, V.; Kluit, R.; van Beuzekom, M.; Zappone, F.; et al. Timepix3: A 65K channel hybrid pixel readout chip with simultaneous ToA/ToT and sparse readout. *J. Instrum.* **2014**, *9*, C05013. [[CrossRef](#)]
 41. Llopart, X.; Aloyz, J.; Ballabriga, R.; Campbell, M.; Casanova, R.; Gromov, V.; Heijne, E.H.M.; Poikela, T.; Santin, E.; Sriskaran, V.; et al. Timepix4, a large area pixel detector readout chip which can be tiled on 4 sides providing sub-200 ps timestamp binning. *J. Instrum.* **2022**, *17*, C01044. [[CrossRef](#)]
 42. van der Graaf, H. GridPix: An integrated readout system for gaseous detectors with a pixel chip as anode. *Nucl. Instrum. Methods Phys. Res. A* **2007**, *580*, 1023–1026. [[CrossRef](#)]

43. Ligtenberg, C.; Heijhoff, K.; Bilevych, Y.; Desch, K.; van der Graaf, H.; Hartjes, F.; Kaminski, J.; Kluit, P.M.; Raven, G.; Schiffer, T.; et al. Performance of a GridPix detector based on the Timepix3 chip. *Nucl. Instrum. Methods Phys. Res. A* **2018**, *908*, 18–23. [[CrossRef](#)]
44. Feng, H.; Liu, H.; Liu, S.; Song, H.; Xie, Y.; Fan, Z.; Chen, S.; Xie, F.; Yan, B.; Liang, E. Charging-up effects for Gas Microchannel Plate detector. *Nucl. Instrum. Methods Phys. Res. A* **2023**, *1055*, 168499. [[CrossRef](#)]
45. Krawczynski, H.; Garson, A.; Guo, Q.; Baring, M.G.; Ghosh, P.; Beilicke, M.; Lee, K. Scientific prospects for hard X-ray polarimetry. *Astropart. Phys.* **2011**, *34*, 550–567. [[CrossRef](#)]
46. Gianolli, V.E.; Kim, D.E.; Bianchi, S.; Agís-González, B.; Madejski, G.; Marin, F.; Marinucci, A.; Matt, G.; Middei, R.; Petrucci, P.O.; et al. Uncovering the geometry of the hot X-ray corona in the Seyfert galaxy NGC 4151 with IXPE. *Mon. Not. R. Astron. Soc.* **2023**, *523*, 4468–4476. [[CrossRef](#)]
47. Ursini, F.; Marinucci, A.; Matt, G.; Bianchi, S.; Marin, F.; Marshall, H.L.; Middei, R.; Poutanen, J.; Rogantini, D.; De Rosa, A.; et al. Mapping the circumnuclear regions of the Circinus galaxy with the Imaging X-ray Polarimetry Explorer. *Mon. Not. R. Astron. Soc.* **2023**, *519*, 50–58. [[CrossRef](#)]
48. Marin, F.; Marinucci, A.; Laurenti, M.; Kim, D.E.; Barnouin, T.; Di Marco, A.; Ursini, F.; Bianchi, S.; Ravi, S.; Marshall, H.L.; et al. X-ray polarization measurement of the gold standard of radio-quiet active galactic nuclei: NGC 1068. *arXiv* **2024**, arXiv:2403.02061. [[CrossRef](#)]
49. Goosmann, R.W.; Matt, G. Spotting the misaligned outflows in NGC 1068 using X-ray polarimetry. *Mon. Not. R. Astron. Soc.* **2011**, *415*, 3119–3128. [[CrossRef](#)]
50. Grefenstette, B.W.; Reynolds, S.P.; Harrison, F.A.; Humensky, T.B.; Boggs, S.E.; Fryer, C.L.; DeLaney, T.; Madsen, K.K.; Miyasaka, H.; Wik, D.R.; et al. Locating the Most Energetic Electrons in Cassiopeia A. *Astrophys. J.* **2015**, *802*, 15. [[CrossRef](#)]
51. Götz, D.; Mereghetti, S.; Tiengo, A.; Esposito, P. Magnetars as persistent hard X-ray sources: INTEGRAL discovery of a hard tail in SGR 1900+14. *Astron. Astrophys.* **2006**, *449*, L31–L34. [[CrossRef](#)]
52. Makishima, K.; Enoto, T.; Yoneda, H.; Odaka, H. A NuSTAR confirmation of the 36 ks hard X-ray pulse-phase modulation in the magnetar 1E 1547.0 - 5408. *Mon. Not. R. Astron. Soc.* **2021**, *502*, 2266–2284. [[CrossRef](#)]
53. Doroshenko, V.; Poutanen, J.; Tsygankov, S.S.; Suleimanov, V.F.; Bachetti, M.; Caiazzo, I.; Costa, E.; Di Marco, A.; Heyl, J.; La Monaca, F.; et al. Determination of X-ray pulsar geometry with IXPE polarimetry. *Nat. Astron.* **2022**, *6*, 1433–1443. [[CrossRef](#)]
54. Mészáros, P.; Novick, R.; Szentgyorgyi, A.; Chanan, G.A.; Weisskopf, M.C. Astrophysical implications and observational prospects of X-ray polarimetry. *Astrophys. J.* **1988**, *324*, 1056. [[CrossRef](#)]
55. Caiazzo, I.; Heyl, J. Polarization of accreting X-ray pulsars. I. A new model. *Mon. Not. R. Astron. Soc.* **2021**, *501*, 109–128. [[CrossRef](#)]
56. Caiazzo, I.; Heyl, J. Polarization of accreting X-ray pulsars. II. Hercules X-1. *Mon. Not. R. Astron. Soc.* **2021**, *501*, 129–136. [[CrossRef](#)]
57. Muleri, F.; Soffitta, P.; Bellazzini, R.; Brez, A.; Costa, E.; Fabiani, S.; Frutti, M.; Minuti, M.; Negri, M.B.; Pascale, P.; et al. A very compact polarizer for an X-ray polarimeter calibration. In *UV, X-ray, and Gamma-Ray Space Instrumentation for Astronomy XV*; SPIE: Bellingham, WA, USA, 2007; Volume 6686, p. 668610. [[CrossRef](#)]
58. Fabiani, S.; Bellazzini, R.; Berrilli, F.; Brez, A.; Costa, E.; Minuti, M.; Muleri, F.; Pinchera, M.; Rubini, A.; Soffitta, P.; et al. Performance of an Ar-DME imaging photoelectric polarimeter. In *Proceedings of the Society of Photo-Optical Instrumentation Engineers (SPIE) Conference Series*; SPIE: Bellingham, WA, USA, 2012; Volume 8443. [[CrossRef](#)]
59. Soffitta, P.; Costa, E.; Muleri, F.; Campana, R.; Del Monte, E.; di Cosimo, S.; Evangelista, Y.; Fabiani, S.; Feroci, M.; Lazzarotto, F.; et al. A set of X-ray polarimeters for the New Hard X-ray Imaging and Polarimetric Mission. In *Proceedings of the Society of Photo-Optical Instrumentation Engineers (SPIE) Conference Series*; SPIE: Bellingham, WA, USA, 2010; Volume 7732. [[CrossRef](#)]
60. Takeda, T.; Black, K.; Enoto, T.; Hayato, A.; Hill, J.; Iwakiri, W.; Jahoda, K.; Kitaguchi, T.; Okubo, M.; Tamagawa, T.; et al. Development and performance verification of a TPC polarimeter for high energy X-rays. In *Proceedings of the Space Telescopes and Instrumentation 2020: Ultraviolet to Gamma Ray*; Society of Photo-Optical Instrumentation Engineers (SPIE) Conference Series; den Herder, J.W.A., Nikzad, S., Nakazawa, K., Eds.; SPIE: Bellingham, WA, USA, 2020; Volume 11444, p. 114445Y. [[CrossRef](#)]
61. Tagliaferri, G.; Hornstrup, A.; Huovelin, J.; Reglero, V.; Romaine, S.; Rozanska, A.; Santangelo, A.; Stewart, G. The NHXM observatory. *Exp. Astron.* **2012**, *34*, 463–488. [[CrossRef](#)]
62. Abarr, Q.; Baring, M.; Beheshtipour, B.; Beilicke, M.; de Geronimo, G.; Dowkontt, P.; Errando, M.; Guarino, V.; Iyer, N.; Kislat, F.; et al. Observations of a GX 301-2 Apastron Flare with the X-Calibur Hard X-ray Polarimeter Supported by NICER, the Swift XRT and BAT, and Fermi GBM. *Astrophys. J.* **2020**, *891*, 70. [[CrossRef](#)]
63. Abarr, Q.; Awaki, H.; Baring, M.G.; Bose, R.; De Geronimo, G.; Dowkontt, P.; Errando, M.; Guarino, V.; Hattori, K.; Hayashida, K.; et al. XL-Calibur—A second-generation balloon-borne hard X-ray polarimetry mission. *Astropart. Phys.* **2021**, *126*, 102529. [[CrossRef](#)]
64. Hayashida, K.; Kim, J.; Sadamoto, M.; Yoshinaga, K.; Gunji, S.; Mihara, T.; Kishimoto, Y.; Kubo, H.; Mizuno, T.; Takahashi, H.; et al. Hard X-ray imaging polarimeter for PolariS. In *Proceedings of the Space Telescopes and Instrumentation 2016: Ultraviolet to Gamma Ray*; Society of Photo-Optical Instrumentation Engineers (SPIE) Conference Series; den Herder, J.W.A., Takahashi, T., Bautz, M., Eds.; SPIE: Bellingham, WA, USA, 2016; Volume 9905, p. 99051A. [[CrossRef](#)]

65. Krawczynski, H.S.; Stern, D.; Harrison, F.A.; Kislak, F.F.; Zajczyk, A.; Beilicke, M.; Hoormann, J.; Guo, Q.; Endsley, R.; Ingram, A.R.; et al. X-ray polarimetry with the Polarization Spectroscopic Telescope Array (PoSTAR). *Astropart. Phys.* **2016**, *75*, 8–28. [[CrossRef](#)]
66. Costa, E.; Cinti, M.N.; Feroci, M.; Matt, G.; Rapisarda, M. Design of a scattering polarimeter for hard X-ray astronomy. *Nucl. Instrum. Methods Phys. Res. A* **1995**, *366*, 161–172. [[CrossRef](#)]
67. Del Monte, E.; Fabiani, S.; Pearce, M. Compton Polarimetry. In *Handbook of X-ray and Gamma-Ray Astrophysics*; Bambi, C., Santangelo, A., Eds.; Springer: Berlin/Heidelberg, Germany, 2023; p. 127. [[CrossRef](#)]
68. Costa, E. Scattering Polarimetry in the Hard X-ray Range. *Instruments* **2024**, *8*, 20. [[CrossRef](#)]
69. Fabiani, S.; Campana, R.; Costa, E.; Del Monte, E.; Muleri, F.; Rubini, A.; Soffitta, P. Characterization of scatterers for an active focal plane Compton polarimeter. *Astropart. Phys.* **2013**, *44*, 91–101. [[CrossRef](#)]
70. Kaaret, P.E.; Schwartz, J.; Soffitta, P.; Dwyer, J.; Shaw, P.S.; Hanany, S.; Novick, R.; Sunyaev, R.; Lapshov, I.Y.; Silver, E.H.; et al. Status of the stellar X-ray polarimeter for the Spectrum-X-Gamma mission. In *Proceedings of the Society of Photo-Optical Instrumentation Engineers (SPIE) Conference Series*; Fineschi, S., Ed.; SPIE: Bellingham, WA, USA, 1994; Volume 2010, pp. 22–27.
71. Maeda, Y.; Abarr, Q.; Awaki, H.; Baring, M.; Bose, R.; Braun, D.; De Geronimo, G.; Dowkontt, P.; Elliot, J.W.; Enoto, T.; et al. XL-Calibur: The next-generation balloon-borne hard X-ray polarimeter. In *Proceedings of the Space Telescopes and Instrumentation 2020: Ultraviolet to Gamma Ray*; Society of Photo-Optical Instrumentation Engineers (SPIE) Conference Series; den Herder, J.W.A., Nikzad, S., Nakazawa, K., Eds.; SPIE: Bellingham, WA, USA, 2020; Volume 11444, p. 114442X. [[CrossRef](#)]
72. Iyer, N.K.; Kiss, M.; Pearce, M.; Stana, T.A.; Awaki, H.; Bose, R.G.; Dasgupta, A.; De Geronimo, G.; Gau, E.; Hakamata, T.; et al. The design and performance of the XL-Calibur anticoincidence shield. *Nucl. Instrum. Methods Phys. Res. A* **2023**, *1048*, 167975. [[CrossRef](#)]
73. Chattopadhyay, T.; Vadawale, S.V.; Goyal, S.K.; Mithun, N.P.S.; Patel, A.R.; Shukla, R.; Ladiya, T.; Shanmugam, M.; Patel, V.R.; Ubale, G.P. Development of a hard X-ray focal plane compton polarimeter: A compact polarimetric configuration with scintillators and Si photomultipliers. *Exp. Astron.* **2016**, *41*, 197–214. [[CrossRef](#)]
74. Elsner, R.F.; Weisskopf, M.C.; Kaaret, P.; Novick, R.; Silver, E. Off-axis effects on the performance of a scattering polarimeter at the focus of an X-ray telescope. *Opt. Eng.* **1990**, *29*, 767–772. [[CrossRef](#)]
75. Aoyagi, M.; Bose, R.G.; Chun, S.; Gau, E.; Hu, K.; Ishiwata, K.; Iyer, N.K.; Kislak, F.; Kiss, M.; Klepper, K.; et al. Systematic effects on a Compton polarimeter at the focus of an X-ray mirror. *Astropart. Phys.* **2024**, *158*, 102944. [[CrossRef](#)]
76. Muleri, F.; Campana, R.; Borciani, E.; Amati, L.; Costa, E.; De Angelis, N.; Del Monte, E.; Di Marco, A.; Fabiani, S.; Fiorini, M.; et al. In search of the third dimension in Compton X-ray polarimeters. In *Proceedings of the SPIE Astronomical Telescopes + Instrumentation (Space Telescopes and Instrumentation 2024: Ultraviolet to Gamma Ray; Conference 13093)*, Yokohama, Japan, 16–21 June 2024.
77. Jahoda, K.; Krawczynski, H.; Kislak, F.; Marshall, H.; Okajima, T.; Agudo, I.; Angelini, L.; Bachetti, M.; Baldini, L.; Baring, M.; et al. The X-ray Polarization Probe mission concept. *arXiv* **2019**, arXiv:1907.10190. [[CrossRef](#)]
78. Soffitta, P.; Bucciantini, N.; Churazov, E.; Costa, E.; Dovciak, M.; Feng, H.; Heyl, J.; Ingram, A.; Jahoda, K.; Kaaret, P.; et al. A polarized view of the hot and violent universe. *Exp. Astron.* **2021**, *51*, 1109–1141. [[CrossRef](#)]

Disclaimer/Publisher’s Note: The statements, opinions and data contained in all publications are solely those of the individual author(s) and contributor(s) and not of MDPI and/or the editor(s). MDPI and/or the editor(s) disclaim responsibility for any injury to people or property resulting from any ideas, methods, instructions or products referred to in the content.